Eco-Environment & Health 4 (2025) 100123

Contents lists available at ScienceDirect

Eco-Environment & Health

journal homepage: www.journals.elsevier.com/eco-environment-and-health

Original Research Article

Global modeling of photochemical reactions in lake water: A comparison between triplet sensitization and direct photolysis

Luca Carena [a], Ángela García-Gil [b], Javier Marugán [c,d], Davide Vione [a,*]

[a] Dipartimento di Chimica, Università di Torino, Via Pietro Giuria 5, 10125 Torino, Italy
[b] Process Design, Repsol Technology Lab, 28935 Móstoles, Madrid, Spain
[c] Grupo de Ingeniería Química y Ambiental, Universidad Rey Juan Carlos, ESCET, C/Tulipán s/n, 28933 Móstoles, Madrid, Spain
[d] Instituto de Investigación de Tecnologías para la Sostenibilidad, Universidad Rey Juan Carlos, ESCET, C/Tulipán s/n, 28933 Móstoles, Madrid, Spain

ARTICLE INFO

Keywords:
Photochemistry
Water pollution
Surface waters
Organic matter
Water depth
Natural attenuation of contaminants

ABSTRACT

The equivalent monochromatic wavelength (EMW) approximation allowed us to predict the photochemical lifetimes of the lipid regulator metabolite clofibric acid (CLO, triplet sensitization) and of the non-steroidal anti-inflammatory drug diclofenac (DIC, direct photolysis + triplet sensitization) in lakes worldwide. To do so, we used large lake databases that collect photochemically significant parameters such as water depth and dissolved organic carbon, which allow for a preliminary assessment of some photoreactions. Extension to other photoreactions is currently prevented by the lack of important parameters such as water absorption spectrum, suspended solids, nitrate, nitrite, pH, and inorganic carbon on a global scale. It appears that triplet-sensitized CLO photodegradation would be strongly affected by the dissolved organic carbon values of the lake water and, for this reason, it would be fastest in Nordic environments. By contrast, direct photolysis (DIC) would be highly affected by sunlight irradiance and would proceed at the highest rates in the tropical belt. Interestingly, the predicted lifetimes of CLO and DIC are shorter than the residence time of water in the majority of global lake basins, which suggests a high potential for photoreactions to attenuate the two contaminants on a global scale. Photodegradation of DIC and CLO would also be important in waste stabilization ponds, except for elevated latitudes during winter, which makes these basins potentially cost-effective systems for the partial removal of these emerging contaminants from wastewater.

1. Introduction

Photochemical reactions play key roles in the attenuation of bio-recalcitrant contaminants in sunlit freshwaters, thereby contributing to the depollution of aquatic environments from many contaminants of emerging concern (CECs) [1–3]. CECs include many chemicals used in daily life, such as pharmaceuticals, personal care products, fragrances, and metal corrosion inhibitors. These compounds can harm both aquatic life forms and humans [4,5], but they can be photochemically degraded by direct photolysis if they absorb sunlight [6]. At the same time or in the alternative, CECs can undergo indirect photolysis, which is the transformation upon reaction with photochemically produced reactive intermediates (PPRIs). PPRIs include the hydroxyl radical $^{\bullet}OH$, carbonate radical $CO_3^{\bullet-}$, singlet oxygen $^1O_2$, and the excited triplet states of the chromophoric dissolved organic matter, $^3CDOM^*$ [7]. Environmental parameters such as depth, organic matter, some dissolved ions, latitude, and season can significantly affect photochemical degradation kinetics, which also differ between seawater and freshwaters [8].

PPRIs are generated upon radiation absorption by photosensitizers, *i.e.*, naturally occurring compounds (for instance, NO_3^-, NO_2^-, and CDOM) that absorb sunlight in the UV-visible region. In particular, the photolysis of both NO_3^- and NO_2^- yields $^{\bullet}OH$ [9], CDOM irradiation produces $^3CDOM^*$, $^1O_2$, as well as $^{\bullet}OH$ [10–12], while $CO_3^{\bullet-}$ is generated upon HCO_3^-/CO_3^{2-} oxidation by $^{\bullet}OH$ and upon CO_3^{2-} oxidation by $^3CDOM^*$ [13,14]. Note that CDOM is partly made up of complexes between Fe(III) and organic ligands, which contribute to PPRI generation, including $^{\bullet}OH$ [15]. Other than being generated, PPRIs are quickly scavenged/quenched upon reaction with DOM (dissolved organic matter), HCO_3^-, and CO_3^{2-} ($^{\bullet}OH$), DOM alone ($CO_3^{\bullet-}$), internal conversion and O_2 reaction ($^3CDOM^*$), as well as collision with the water solvent

* Corresponding author.
E-mail address: davide.vione@unito.it (D. Vione).

https://doi.org/10.1016/j.eehl.2024.09.001
Received 3 April 2024; Received in revised form 16 July 2024; Accepted 10 September 2024
Available online 19 September 2024

($^1O_2$) [10,16,17]. Moreover, in seawater, Br^- is the main $^\bullet OH$ scavenger [18]. The budget between photogeneration and scavenging/quenching results in PPRIs reaching very low steady-state concentrations under sunlight, typically in the 10^{-18}–10^{-14} M range, often following the order $^\bullet OH < {}^3CDOM^* \approx {}^1O_2 < CO_3^{\bullet-}$. In particular, $^\bullet OH$, $CO_3^{\bullet-}$, and the direct photolysis are usually enhanced in DOM-poor waters (containing low dissolved organic carbon, *i.e.*, DOC), while the opposite happens for processes triggered by $^3CDOM^*$ and $^1O_2$ [7].

It is now possible to reliably model the kinetics of aquatic photoreactions, and several models and/or software packages have been developed for this purpose [19–22]. A recently developed expert system is even able to predict the direct photolysis products of contaminants [23,24]. The packages that predict photoreaction kinetics are based on multi-wavelength calculations, which take into account the polychromatic nature of both sunlight and the radiation absorption by photosensitizers and contaminants [25]. Moreover, a monochromatic approximation has been developed recently that highly simplifies the mathematics involved in kinetic calculations. This approach is based on the equivalent monochromatic wavelength (EMW or λ_{eq}) and consists in finding the wavelength that alone approximates the polychromatic system [26]. The EMW approach has paved the way for the assessment of photoreaction kinetics on a wide geographic scale [27,28]. To do so, however, one needs an easy way to assess the global sunlight irradiance at λ_{eq} and, preferably, its seasonal variations as well. We recently succeeded in reaching this goal, at least for the 60°S–60°N latitude belt [27]. The final issue is the availability of global water chemistry data; while a global database of full chemical water parameters is not yet available, there are global estimates of lake-water DOC and depth [29,30] that are the most significant parameters for photochemical reaction kinetics.

In this work, we carry out a global-scale comparison of the photochemical behavior of two contaminants of emerging concern that differ for the prevailing phototransformation pathways, namely clofibric acid ($^3CDOM^*$ reaction) and diclofenac (direct photolysis plus $^3CDOM^*$ reaction). The presence of both clofibric acid and diclofenac in all the study lakes is adopted here as a hypothetical scenario for a geographical comparison of the direct photolysis and $^3CDOM^*$-induced reactions. We can thus provide insight into the global significance of these processes, the locations where either prevails, and the associated lifetimes of the investigated pollutants. Such pieces of information play a key role in the assessment of the photochemical depollution potential of freshwaters and, in turn, allow for the identification of environments that are most vulnerable to pollution as an important tool for freshwater management.

2. Methods

2.1. Lakes considered in the photochemical model

Data about dissolved organic carbon (DOC) of lake water were obtained from the work of Toming and co-workers [30,31]. Toming et al. have used a machine-learning technique and global databases to estimate DOC in lakes with a surface area > 0.1 km^2. Catchment properties, meteorological and hydrological features, as well as lake morphometry were used as input data for the model [30]. Data on global lakes and reservoirs were obtained from HydroLAKES v. 1.0 21 [29,32], available at the website https://www.hydrosheds.org (Accessed January 2024). HydroLAKES contains data about 1.43 million individual lakes, including both fresh- and saline waters, with a surface area of at least 0.1 km^2 [29,32]. For the lakes considered in the present study, the DOC had an average relative standard deviation of 20% that was assessed by uncertainty data on the predicted DOC values, as reported in the database of Toming and co-workers [30,31].

For the purposes of the present photochemical modeling/mapping, only a small fraction of the lakes included in the HydroLAKES + Toming's work databases were considered based on geographical coordinates, average lake-water depth, and ground altitude. The latitude belt >60°N was not considered because (i) our solar photon-flux model is not valid for that region, and (ii) ice/snow coverage of lakes can be a problem for the photochemical model, especially in the cold season. Only those lakes with an average water depth ≥5 m were chosen, which would limit issues connected with the high turbidity of shallow water bodies during overturn. The photochemical model was run using the value of the average lake-water depth reported in HydroLAKES, which is defined as the ratio between total lake volume and lake area [32]. Most of the considered lakes (~86%) have an average depth between 5 and 10 m, while for an additional ~13% the average depth is between 10 and 50 m. The remaining 1% has an average depth ≥ 50 m. Since the predictions of our photochemical model are good in the water-depth range between 5 and 50 m (*vide infra*), computations for lakes with depth > 50 m were run by setting 50 m as the water-column depth.

Regarding altitude (h), only lakes located at h < 500 m a.s.l. were considered in our model. Lakes located at elevations ≥ 500 m a.s.l. (~11% of the total) were excluded because the model does not consider: (i) the ice/snow coverage of lakes, possibly occurring in some regions of the world (*e.g.*, alpine areas of temperate regions), and (ii) the variability of the solar photon flux with ground elevation for some geographical conditions. Despite the fact that altitude-related sunlight spectrum might not be that important for several aquatic photoreactions [33], in some cases (and especially for some compounds undergoing direct photolysis), the spectral variations can be similar to or slightly higher than seasonal variations in solar-photon-flux models [34]. The database was thus reduced to 72,380 lakes (~5% of the lake number present in the HydroLAKES database).

2.2. Assessment of $^3CDOM^*$ concentration

The values of the steady-state concentration of $^3CDOM^*$ ($C_{^3CDOM^*}$, units of mol/L) were computed for the considered 72,380 lakes, as follows:

$$C_{^3CDOM^*} = \frac{10\eta_{app(560\ nm)}p^\circ_{(560\ nm)}}{dk'_d}\left[1 - 10^{-\frac{100A_{1(560\ nm)}C_{DOC}d}{n}}\right]^a \quad (1)$$

where: 10 is the conversion factor between units of ($m^{-1}\bullet cm^{-2}$) and (L^{-1}); 100 is the conversion factor between units of m and cm; $\eta_{app(560\ nm)}$ = 0.46 mol nm/E (E = Einstein = mole of photons) is the photon efficiency for $^3CDOM^*$ formation from irradiated CDOM [26]; $p^\circ_{(560\ nm)}$ is the photon flux density of sunlight at 560 nm [units of E/(cm^2·s·nm)] [20]; d is the lake-water depth (units of m; see the previous section for its values); $k'_d = 5 \times 10^5\ s^{-1}$ is the pseudo-first order rate constant of $^3CDOM^*$ quenching by O_2 in aerated solution [10]; $A_{1(560\ nm)} = 1 \times 10^{-4}$ L/(mg_C·cm) is an average value for the 560-nm absorption coefficient of CDOM [26]; C_{DOC} is the lake-water DOC in mg_C/L, the values of which were from refs. [30,31]; n = 5.40 and a = 0.35 are parameters derived from EMW validation (*vide infra*).

The values of $A_{1(560\ nm)}$, k_d, and $\eta_{app(560\ nm)}$ are reasonable averages, but the photoactivity of CDOM may vary depending on its sources. For instance, there is some evidence that pedogenic organic matter is more reactive overall (i.e., considering both sunlight absorption and photon efficiencies) than the aquagenic one [35].

2.3. Computing clofibric acid (CLO) photodegradation in the studied lakes

The $^3CDOM^*$ concentrations were used to compute parameters relative to the indirect photodegradation of CLO in the considered lakes. It should be pointed out that CLO can be degraded by both $^3CDOM^*$ and $^\bullet OH$ [36–38], but our model cannot take the latter reaction into account because of a lack of data about the global distribution of $^\bullet OH$ photosensitizers other than CDOM (mainly, nitrate and nitrite). The pseudo-first order rate coefficient of CLO photodegradation by $^3CDOM^*$ (k'_{CLO}, units of day^{-1}) was computed as $k'_{CLO} = 3600\psi k_{CLO+{}^3CDOM^*}C_{^3CDOM^*}\tau_{DL}$, where $k_{CLO+{}^3CDOM^*} = 5.23 \times 10^9$ L/(mol·s) is the bimolecular rate constant of the reaction between CLO and $^3CDOM^*$, assessed by using the triplet state of

benzophenone-4-carboxylate as ^{3}CDOM* surrogate [38]. Such relatively high reactivity is likely due to the fact that CLO is a phenolic ether, and phenolic compounds are quite reactive towards ^{3}CDOM* [10]. The parameter $\tau_{DL} = \frac{2}{15}\arccos(-\tan\phi\tan\delta)$ is the day length in hours (note that the value of the arccos is in degrees) [27]; δ is the Sun's declination expressed as $\delta = 23.45° \sin\left[\frac{360}{365}(day + 284)\right]$, where $day = 1$ is 1st January and $day = 365$ is 31st December, and 60°S ($-60°$) < ϕ < 60°N (+60°) is the latitude [27]. Since CLO oxidation by ^{3}CDOM* can be inhibited by the antioxidant moieties of DOM [38], the parameter $\psi = 0.68 + 0.32/(1 + 10C_{DOC})$ was introduced here to take this inhibition effect into account [38–40]. Finally, 3600 is the conversion factor between seconds and hours (1 h = 3600 s). The photochemical half-life time of CLO in lake water was assessed as $t_{1/2} = \ln 2/k'_{CLO}$.

2.4. Computing diclofenac (DIC) photodegradation in the considered lakes

Although DIC can undergo direct photolysis as well as oxidation by ^{3}CDOM* and $^\bullet$OH, the $^\bullet$OH reaction would account for no more than 10% of the overall DIC photodegradation for DOC values ranging between 1 and 10 mg$_C$/L [37]. On the contrary, direct photolysis is the main phototransformation pathway for DIC in surface waters, followed by ^{3}CDOM* [37,41].

Here, the rate coefficient of DIC direct photolysis ($k'_{DIC,d.p.}$, units of day^{-1}) in lake water was computed as follows:

$$k'_{DIC,d.p.} = \frac{36000 p^\circ_{(315\ nm)} \eta_{app(315\ nm)} \varepsilon_{DIC(315\ nm)} \tau_{DL}}{d A_{1(315\ nm)} C_{DOC}} \left(1 - 10^{-100 A_{1(315\ nm)} C_{DOC} d}\right) \quad (2)$$

where: 36,000 is the conversion factor between units of (L/h) and (m•cm^2/s); $p^\circ_{(315\ nm)}$ is the photon flux density of sunlight at 315 nm [units of E/(cm^2·s·nm)] [20]; $\eta_{app(315\ nm)} = 1.34$ mol nm/E is the photon efficiency of DIC direct photolysis [26]; $\varepsilon_{DIC(315\ nm)} = 583$ L/(mol·cm) is the molar absorption coefficient of DIC at 315 nm [20]; τ_{DL} is the day length (h/day) as previously described; d is the lake-water depth (m); $A_{1(315\ nm)} = 4 \times 10^{-3}$ L/(mg$_C$·cm) is an average value for the 315-nm absorption coefficient of CDOM [20]; C_{DOC} is the DOC value in mg$_C$/L, taken from refs. [30,31].

The pseudo-first order rate coefficient of DIC degradation by ^{3}CDOM* (units of day^{-1}) was computed as $k'_{DIC,^3CDOM*} = 3600\ k_{DIC+^3CDOM*} C_{^3CDOM*}\ \tau_{DL}$, where $k_{DIC+^3CDOM*} = 1 \times 10^9$ L/(mol·s) is the bimolecular rate constant of the reaction between DIC and ^{3}CDOM* [37]. The photochemical half-life time of DIC (units of days) was assessed as $t_{1/2} = \ln 2/(k'_{DIC,d.p.} + k'_{DIC,^3CDOM*})$.

2.5. Model validation

First of all, the monochromatic approximation for ^{3}CDOM* concentration (Eq. 1) was compared with the multi-wavelength assessment of the same quantity. The integral equation for ^{3}CDOM* concentration reads as follows [26]:

$$C_{^3CDOM*} = \frac{10}{d k_d} \int_\lambda \Phi_{^3CDOM*}\ p^\circ(\lambda) \left[1 - 10^{-100 A_1(\lambda) C_{DOC} d}\right] d\lambda \quad (3)$$

where most variables have already been described when introducing Eq. 1. Here, as a difference from Eq. 1, the sunlight photon flux density $p^\circ(\lambda)$ and water absorbance $A_1(\lambda)$ are wavelength-dependent. In Fig. 1a, the concentrations of ^{3}CDOM* with varying DOC (with DOC = C_{DOC}) and water depth d are represented as squares when calculated according to Eq. 3, while the dashed curves represent the fit of the multi-wavelength data with the monochromatic Eq. 1 (which, among other things, allowed for the determination of the n and a parameters).

A similar issue applies to the case of $k'_{DIC,d.p.}$, where the polychromatic assessment (Eq. 4) [26] was fitted with the monochromatic Eq. 2. The fit results are shown in Fig. 1b.

$$k'_{DIC,d.p.} = \frac{36000 \tau_{DL}}{d C_{DOC}} \int_\lambda \frac{p^\circ(\lambda) \Phi_{DIC} \varepsilon_{DIC}(\lambda)}{A_1(\lambda)} \left[1 - 10^{-100 A_1(\lambda) d C_{DOC}}\right] d\lambda \quad (4)$$

In both cases (Fig. 1a and b), there was excellent agreement between the polychromatic data and the monochromatic approximation.

The next step was to compute $p^\circ_{(315\ nm)}$ and $p^\circ_{(560\ nm)}$ as a function of the day and latitude. In the case of λ = 560 nm, the daily dose reaching the Earth's surface was computed as follows [27]:

$$G_{day(560\ nm)} = F_1 p^\circ_{sn(560\ nm)} \tau_{DL} = \int_{1\ day} p^\circ_{(560\ nm,t)} dt \quad (5)$$

where $p^\circ_{sn(560\ nm)} = I_{AM0(560\ nm)} \exp\left[\frac{-\kappa_{(560\ nm)}}{\cos(\phi-\delta)+0.506\times(96.08+\phi-\delta)^{-1.636}}\right] \frac{560}{hcN_a}$ [units of E/(cm^2·s·nm)] is the incident spectral photon flux density of sunlight at solar noon, with I_{AM0} as the intensity of sunlight outside the atmosphere [$(I_{AM0(560\ nm)} = 1.786$ W/(m^2·nm)] [43], κ as the atmospheric extinction coefficient [$\kappa_{(560\ nm)} = 0.128$ AM^{-1}] [43], ϕ as the latitude, h as Planck's constant, c as light's speed in vacuum, and N_a as Avogadro's number.

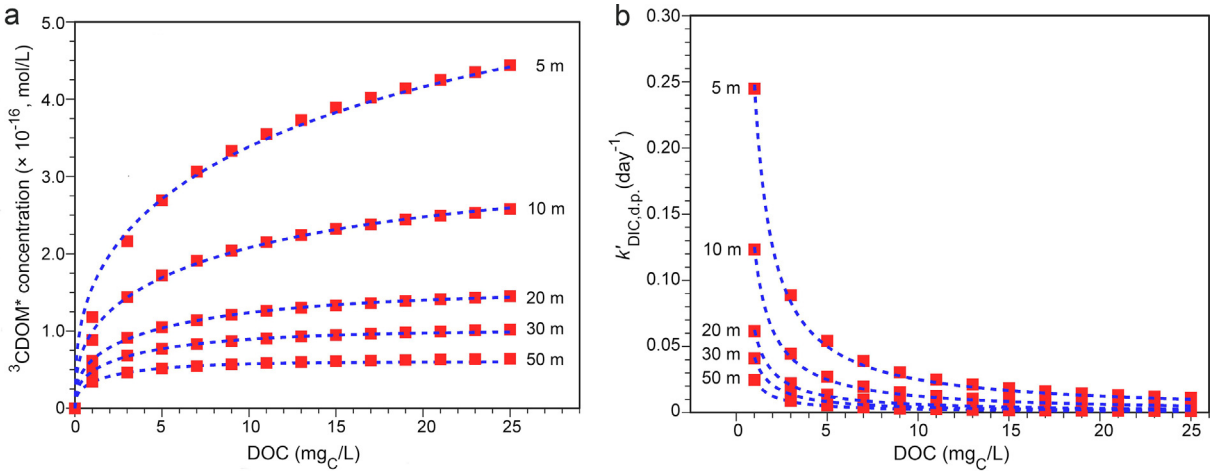

Fig. 1. (a) Calculated steady-state concentrations of ^{3}CDOM* for different values of the water depth (average value, shown near each data series) and the DOC (note that DOC = C_{DOC}). The squares represent polychromatic calculations (Eq. 3), while the dashed curves are the assessments carried out with the EMW approximation (Eq. 1). (b) Calculated values of $k'_{DIC,d.p.}$, for different water depths and DOC values. The squares represent polychromatic calculations (Eq. 4), while the dashed curves are the assessment carried out with the EMW approximation (Eq. 2). Well-mixed water conditions are assumed here. Sunlight irradiance: noon, 45°N, spring equinox.

The expressions used for δ and τ_{DL} were already introduced in *Section 2.3*. As far as the integral in Eq. 5 is concerned, each value of $p^{\circ}_{(560\ nm,\ t)}$ was computed by introducing the zenith angle obtained with the Solar Position Algorithm (SPA) from the National Renewable Energy Laboratory (NREL) [44], for each hour of the day.

By so doing, it is possible to obtain $F_1 = \left[p^{\circ}_{sn(560\ nm)}\tau_{DL}\right]^{-1} \int_{1\ day} p^{\circ}_{(560\ nm,t)}dt$ and to compute $G_{day(560\ nm)}$ for all days and latitudes ($-60^{\circ} < \phi < 60^{\circ}$). The validation of this approximated assessment for $\lambda = 560$ nm has been reported in our previous work [28].

An analogous procedure was carried out in the case of $\lambda = 315$ nm. Fig. 2a shows the fit procedure that allowed us to obtain $F_{1(315\ nm)} = 0.52$ from Eq. 5, in the case of mid-latitude sunlight. Fig. 2b and c shows the very good agreement between both sides of Eq. 5 (exact, integral = solid symbols; approximation = curves), when assuming $F_{1(315\ nm)} = 0.52$ on a worldwide scale.

Overall, the normalized mean root square error between integral and predicted values was <11%. These results suggest that the EMW approximation is suitable for the global modeling of CLO (^{3}CDOM*) and DIC (direct photolysis + ^{3}CDOM*) photodegradation.

2.6. Limits of the model

The used model has limits, some of which are intrinsic while others are caused by a lack of input data. First of all, no worldwide data on nitrate, nitrite, pH, or inorganic carbon in lake water are available, which prevents the modeling of reactions involving $^{\bullet}OH$ or $CO_3^{\bullet-}$. Further, the approach we used is in principle able to deal with stratified lakes, by considering hypolimnion and epilimnion separately [45]. Photoreactions are less efficient in stratified lakes compared to mixing ones [46], although the scenario might change depending on pollution sources [45]. However, no global data are currently available for thermocline depths that would also vary during the year in stratified lakes. Therefore, we assumed here well-mixed water columns and, to minimize uncertainties, the reported data refer to the spring equinox when lake turnover is often active.

No data on water turbidity are available for worldwide lakes, thus we considered radiation absorption only and not scattering by suspended particles. Suspended solids modify the underwater light field by increasing near-surface irradiance and decreasing illumination of the lower depths. Still, unless an important fraction of radiation is reflected towards the sky, the average irradiance in the whole water column is modified less substantially [47]. Our model deals with water-column average values in a mixed system, which limits the impact of scattering on the results. Moreover, we did not consider the shallowest lakes ($d < 5$ m) to minimize turbidity issues.

The type and origin of organic matter would also affect its photoreactivity [35]. Considering that this type of information was not available, here we considered average (C)DOM properties.

Finally, our model considers clear-sky conditions. Cloud cover would decrease photoreaction rates by up to 40%–50% in some equatorial areas and in East Asia [48]. Even larger effects are predicted for Nordic latitudes with $\phi > 60^{\circ}$, but these regions are not included in our model.

2.7. Photochemical mapping

The relevant photochemical parameters (e.g., ^{3}CDOM* concentration and half-life times of CLO and DIC) were mapped by means of the QGIS software (version 3.2.3-Bonn) [42]. For this purpose, the dataset obtained for a given photochemical parameter y was divided into four color-labeled groups, defined by considering the average (μ_y) and standard deviation (σ_y) of that dataset. In particular, the chosen intervals were: (i) $y < \mu_y - \sigma_y$; (ii) $\mu_y - \sigma_y < y < \mu_y$; (iii) $\mu_y < y < \mu_y + \sigma_y$, and (iv) $y > \mu_y + \sigma_y$. In general, for a given parameter y, reddish points indicate higher photochemical activity of lake water, while bluish points suggest lower photochemical activity.

3. Results and discussion

3.1. Global-scale photodegradation processes

The global map of ^{3}CDOM* concentration, computed with the EMW approximation ($\lambda_{eq} = 560$ nm, Eq. 1) for the spring equinox (20th of March) is shown in Fig. 3. On this day, the clear-sky irradiance of sunlight is maximum at the equator and minimum at the poles, and despite this, the highest values of ^{3}CDOM* concentration are predicted at quite high latitudes in the Northern hemisphere. The reason for this finding is that most high-DOC waters are found in Nordic regions [30] (see Figure SM1 in the Supplementary Material for a map of the DOC values used in this work) and, besides irradiance, ^{3}CDOM* concentration has a strong positive correlation with the DOC as well [49].

The global distribution of CLO half-life times [$t_{1/2}$(CLO), Fig. 4a], as driven by the reaction with ^{3}CDOM*, has many similarities with ^{3}CDOM* concentration. Indeed, where ^{3}CDOM* concentration is higher, the half-life time of CLO is shorter. CLO photodegradation would thus be favored in lakes with high DOC values. However, one should consider that $t_{1/2}$(CLO) is also affected by lake-water depth and by the inhibition of the ^{3}CDOM*-induced oxidation of CLO carried out by DOM antioxidant moieties [$\psi = 0.68 + 0.32/(1 + 10C_{DOC})$] [38]. In deep lakes, the half-life time of CLO is longer than in shallow lakes, all other variables being constant, while high DOC means high ^{3}CDOM* concentration and high CLO back-reduction at the same time, where the former is favorable and the latter detrimental to degradation.

It is possible to compare our predicted photodegradation kinetics with the disappearance of CLO in lake water. In a previous field study [50], CLO has been found to undergo photodegradation with first-order rate coefficient $k' \approx 0.01$ day^{-1} in the epilimnion of lake Greinfensee

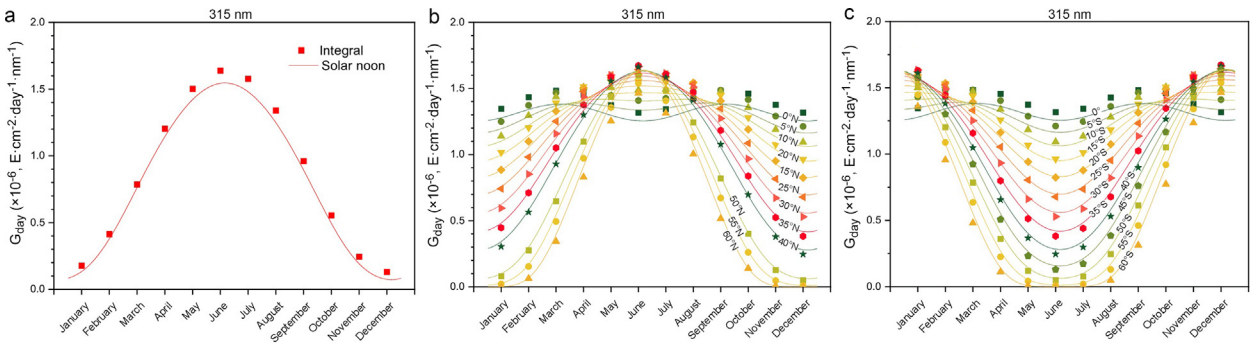

Fig. 2. (a) Fit for the daily dose during the year for a latitude of 45°N. The solid squares represent the values integrated along the 15th day of each month. The solid line shows the values predicted by Eq. 5, with $F_1 = 0.52$. (b,c) Validation of the procedure to calculate the daily dose as a function of the latitude and the day of the year (curves: calculated daily dose; dots: integrated daily dose). (b) Latitudes from 0° to 60°N with steps of 5°. (c) Latitudes from 60°S to 0°.

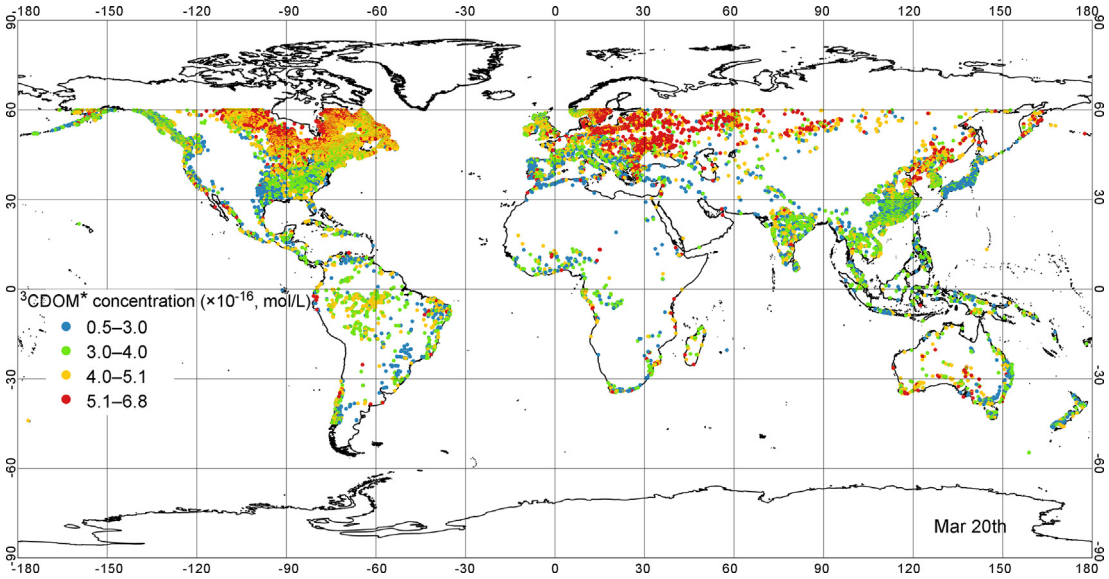

Fig. 3. Global map of the steady-state concentration of ^{3}CDOM* computed for the spring equinox.

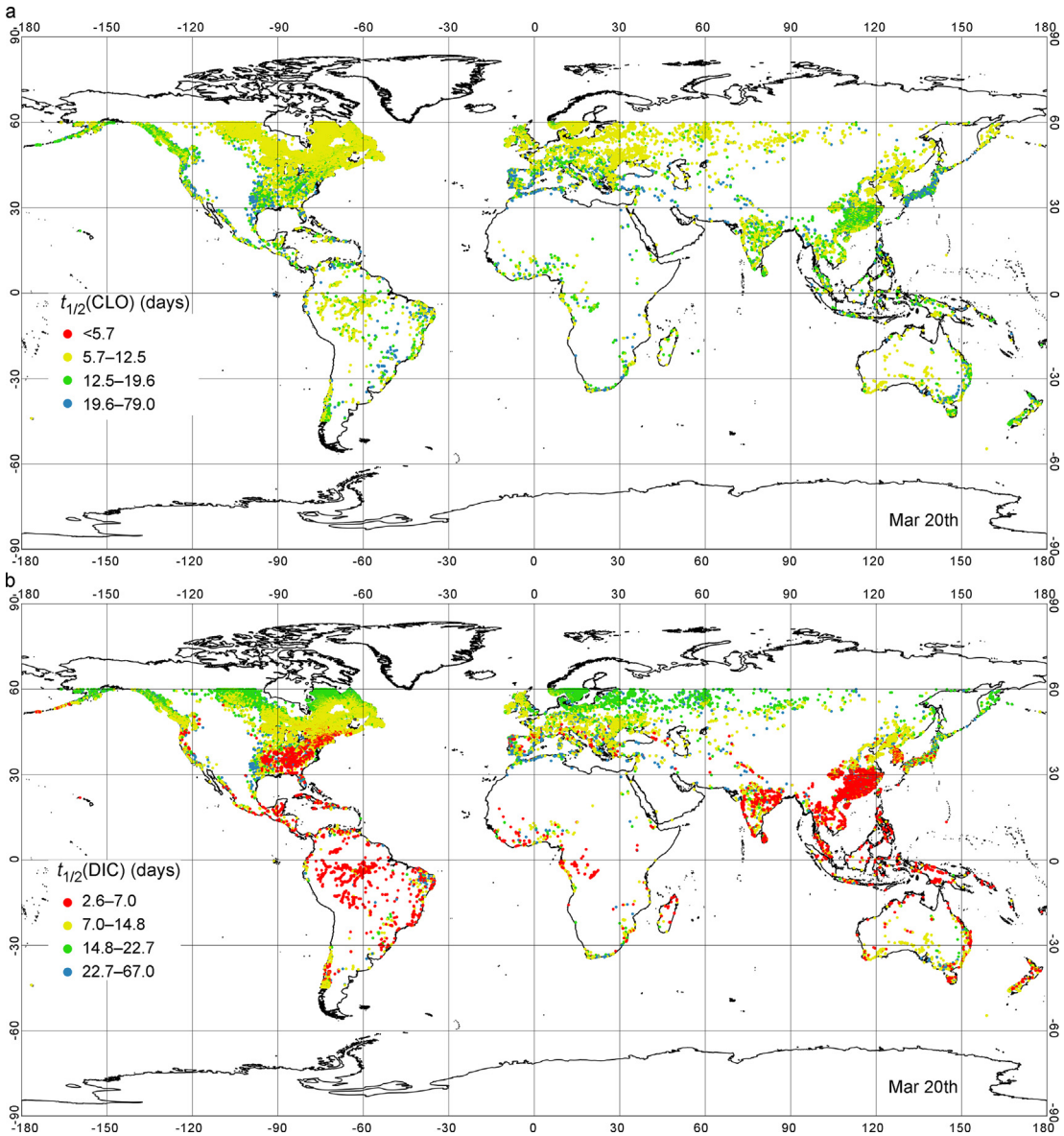

Fig. 4. Global maps of the photochemical half-life times ($t_{1/2}$) of (a) CLO and (b) DIC, computed for the spring equinox.

(Switzerland) in late summer. With our model, for the same depth (10 m), and decreasing irradiance by 1.5 times as reported [50] to account for the cloud cover, we obtained $k' \approx 0.02$ day^{-1}. A factor of 2 difference is quite acceptable when taking into account all the approximations used in our model.

Photodegradation of DIC highlights a similar $t_{1/2}$ range but a different scenario than that of CLO. Fig. 4b shows that DIC photodegradation would be faster in and around the tropical belt, while its rate would decrease [i.e., $t_{1/2}$(DIC) would increase] when moving north or south. This is due to the fact that direct photolysis dominates DIC photodegradation in most conditions, with the exception of high-DOC waters in the northern hemisphere (Fig. 5). In the latter case, the lakes where the contribution of DIC direct photolysis would be lower are characterized by high values of the DOC, which enhance ^{3}CDOM* concentration and inhibit the direct photolysis due to light screening.

Overall, these findings suggest that direct photolysis processes would be much more closely linked to sunlight irradiance than the ^{3}CDOM* reactions, which explains why DIC photodegradation at the equinox would be faster around the equator than at higher northern or southern latitudes.

As previously done with CLO, it is possible to compare the first-order rate coefficient of DIC photodegradation as computed with our model with a field value reported for the epilimnion of lake Greinfensee (Switzerland) in late summer. Tixier et al. [50] found $k' \approx 0.08$ day^{-1}, while our model predicts $k' \approx 0.04$ day^{-1}, still within a factor of 2 difference.

Finally, it is interesting to observe that the average ratios between the computed half-life times of CLO and DIC and the hydraulic residence times of water in the lakes, as reported in the HydroLAKES database [29,32], range between 0.5 and 0.7. This means that, on average, the photodegradation kinetics of CLO and DIC in a lake would be faster than lake-water turnover. Therefore, photodegradation would play an important role in the attenuation of both contaminants in global lake waters.

3.2. Photodegradation processes in waste stabilization ponds

Waste stabilization ponds (WSPs) or treatment lagoons are wastewater treatment facilities intended to serve small communities. They rely

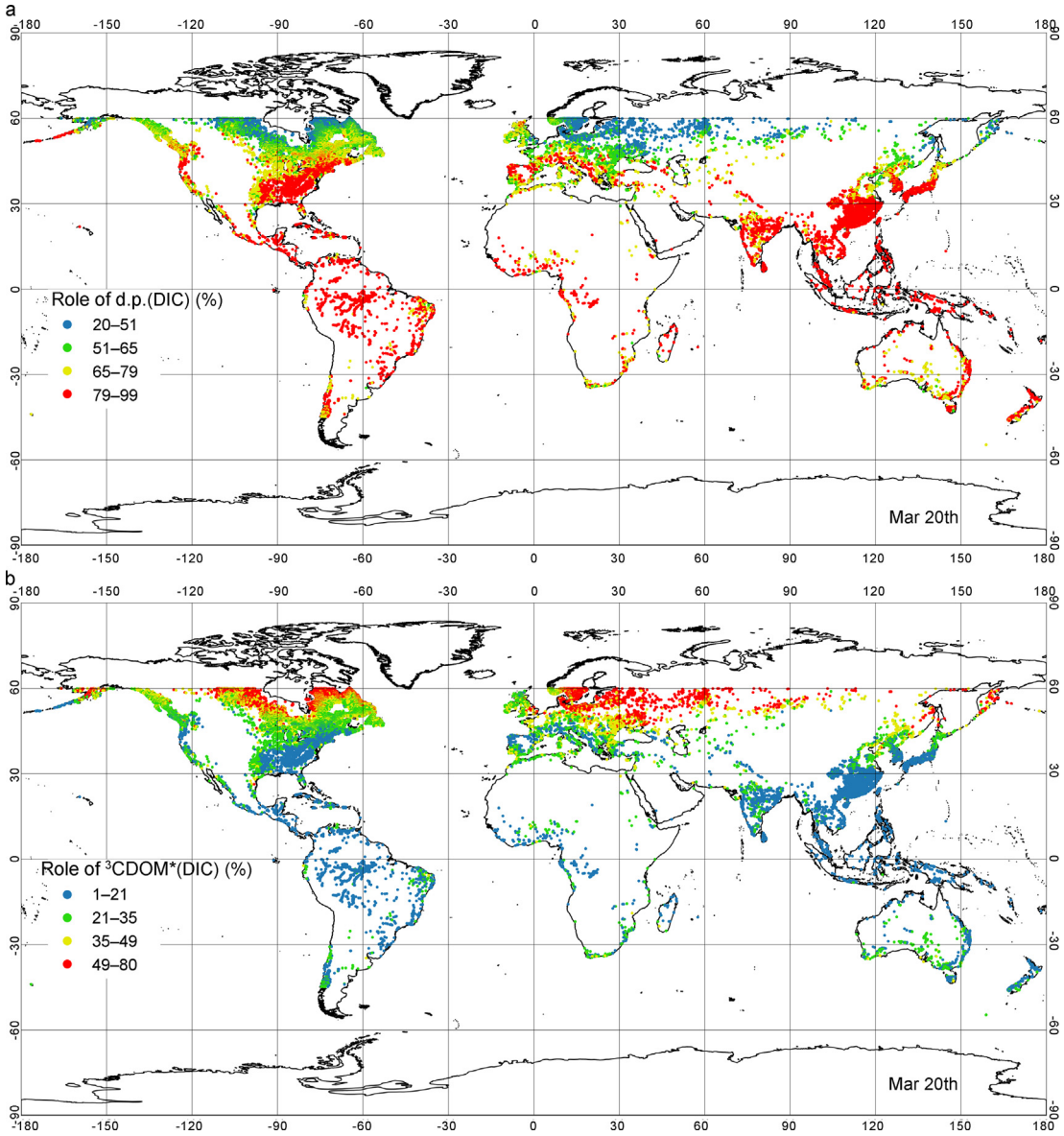

Fig. 5. (a) Contribution of direct photolysis (d.p.), in percentage units [$100k'_{DIC,d.p}/(k'_{DIC,d.p.} + k'_{DIC,^3CDOM*})$], to the overall photodegradation of DIC on the spring equinox. (b) Contribution of ^{3}CDOM*, in percentage units [$100k'_{DIC,^3CDOM*}/(k'_{DIC,d.p.} + k'_{DIC,^3CDOM*})$], to the overall photodegradation of DIC on the spring equinox. Note that blue means limited contribution and red means major contribution, but for the sake of readability, the ranges are not the same in the two figure panels.

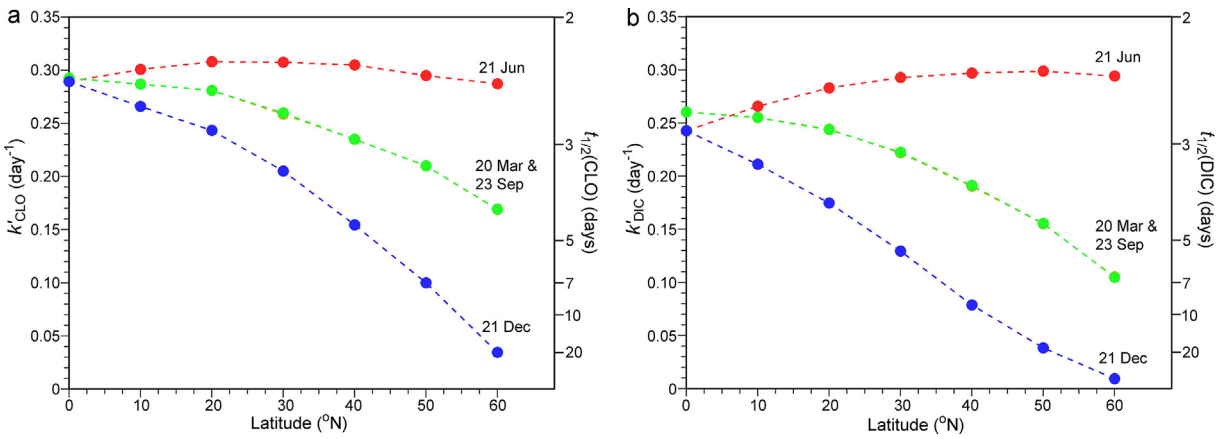

Fig. 6. Modeled first-order photodegradation rate coefficients (k, left Y-axis) and half-life times ($t_{1/2}$, right Y-axis) of (a) CLO (^{3}CDOM* reaction) and (b) DIC (^{3}CDOM* reaction plus direct photolysis) as a function of latitude, at the equinoxes and solstices. Conditions: C_{DOC} = 15 mg$_C$/L, d = 1 m, thorough water mixing, clear sky. Data are referred to the northern hemisphere, but similar results would be obtained for the southern one.

on plants, microorganisms, and sunlight for the removal of nutrients, metals, pathogenic viruses and bacteria, as well as (possibly) organic pollutants [51]. In the case of pollutants, sunlight plays a major role in degradation, and our model approach allows for an assessment of the WSP potential to photochemically remove DIC and CLO on a global scale. WSPs are usually shallow to allow sunlight to illuminate most of the water column and for surface-attached biofilms to be more effective at biodegradation, thus, here we assumed d = 1 m and a typical C_{DOC} = 15 mg$_C$/L [52]. By means of Eqs. 1,2 and with these values of d and C_{DOC}, it is possible to compute ^{3}CDOM* concentration, $k'_{DIC,d.p.}$, and the first-order rate coefficients for degradation of both DIC and CLO by ^{3}CDOM*. The resulting overall, first-order photodegradation rate coefficients are shown in Fig. 6 as a function of season (solstices and equinoxes) and latitude. They are computed for the northern hemisphere, but similar results would be obtained for the southern one.

First of all, as already observed for lake waters as a global average, the half-life times of DIC and CLO (some days in both cases, depending on the season) would be quite similar in WSP conditions. DIC and CLO photodegradation would also be slower by around one order of magnitude compared to the inactivation of pathogenic viruses [52]. In June, when photodegradation of DIC and CLO would be most effective, kinetics would not change much with latitude, unlike in the other months.

By considering a hydraulic retention time of water of 15 days in a typical WSP [51], almost complete photochemical removal of DIC and CLO would take place in June at all latitudes. Under clear-sky conditions, as assumed here, the system would also be fairly effective in March and September. Finally, performance would become rather poor in December at the highest latitudes, and possible cloud cover would slow down photodegradation even further.

Overall, the ability of WSPs to photochemically remove DIC and CLO would depend on hydraulic retention time, latitude, season, and likelihood of fair weather. In many cases, the photoinduced removal would be significant, which makes the use of WSPs a very cost-effective strategy for the attenuation of easily photodegradable CECs.

4. Conclusions

The EMW approximation is suitable for the prediction of both ^{3}CDOM* reactions and direct photolysis on a global scale, as shown here for the emerging contaminants CLO and DIC. The reason for limiting the assessment to triplet sensitization and direct photolysis is also not linked to the EMW approach, but to the lack of data regarding nitrate, nitrite, and inorganic carbon concentrations in lakes globally.

Interestingly, processes mediated by ^{3}CDOM* are strongly linked with the DOC values of water, which are expected to play a more important global role towards ^{3}CDOM* than sunlight irradiance. As a consequence of this, the fastest CLO photodegradation on the spring equinox would be observed at Nordic latitudes instead of the equator where clear-sky sunlight irradiance reaches its maximum values. The opposite happens in the case of direct photolysis, which dominates the photodegradation of DIC and follows irradiance much more closely.

Direct photolysis and ^{3}CDOM* reactions would also play an important role in the attenuation of DIC and CLO in waste stabilization ponds under clear-sky conditions, except for elevated latitudes in winter. Interestingly, at constant DOC, the photodegradation kinetics of DIC and CLO in June would be practically independent of latitude in the absence of cloud cover.

Finally, although a worldwide assessment of $^{\bullet}$OH and $CO_3^{\bullet-}$ processes cannot be obtained yet due to missing data as explained above, the rather strong negative correlation between DOC and $^{\bullet}$OH or especially $CO_3^{\bullet-}$ [7] would suggest that these processes could follow similar or even more marked worldwide trends as the direct photolysis and, for this reason, they could be even more skewed away from Nordic environments.

CRediT authorship contribution statement

Luca Carena: Writing – review & editing, Writing – original draft, Validation, Methodology, Investigation, Formal analysis, Data curation. **Ángela García-Gil:** Writing – review & editing, Writing – original draft, Validation, Methodology, Investigation. **Javier Marugán:** Writing – review & editing, Resources, Funding acquisition. **Davide Vione:** Writing – review & editing, Supervision, Software, Funding acquisition, Conceptualization.

Declaration of competing interests

The authors declare that they have no known competing financial interests or personal relationships that could have appeared to influence the work reported in this paper.

Acknowledgements

JM gratefully acknowledges the financial support of the Spanish State Research Agency (AEI), the Spanish Ministry of Science and Innovation through the project AQUAENAGRI (PID2021-126400OB-C32). LC and DV acknowledge support from the Project CH4.0 under the MUR program "Dipartimenti di Eccellenza 2023–2027" (CUP: D13C22003520001). DV also acknowledges financial support by European Union, Next Generation EU, Mission 4, Component 2, in the framework of the project GRINS, Growing Resilient, INclusive, and Sustainable (GRINS PE00000018, CUP D13C22002160001).

Appendix A. Supplementary data

Supplementary data to this article can be found online at https://doi.org/10.1016/j.eehl.2024.09.001.

References

[1] K. Fenner, S. Canonica, L.P. Wackett, M. Elsner, Evaluating pesticide degradation in the environment: blind spots and emerging opportunities, Science 341 (2013) 752–758, https://doi.org/10.1126/science.1236281.

[2] E. Koumaki, D. Mamais, C. Noutsopoulos, M.-C. Nika, A.A. Bletsou, N.S. Thomaidis, A. Eftaxias, G. Stratogianni, Degradation of emerging contaminants from water under natural sunlight: the effect of season, pH, humic acids and nitrate and identification of photodegradation by-products, Chemosphere 138 (2015) 675–681, https://doi.org/10.1016/j.chemosphere.2015.07.033.

[3] C.K. Remucal, The role of indirect photochemical degradation in the environmental fate of pesticides: a review, Environ. Sci. Process. Impacts 16 (2014) 628–653, https://doi.org/10.1039/c3em00549f.

[4] R.P. Schwarzenbach, B.I. Escher, K. Fenner, T.B. Hofstetter, C.A. Johnson, U. von Gunten, B. Wehrli, The challenge of micropollutants in aquatic systems, Science 313 (2006) 1072–1077, https://doi.org/10.1126/science.1127291.

[5] D. Yadav, S. Rangabhashiyam, P. Verma, P. Singh, P. Devi, P. Kumar, C.M. Hussain, G.K. Gaurav, K.S. Kumar, Environmental and health impacts of contaminants of emerging concerns: recent treatment challenges and approaches, Chemosphere 272 (2021) 129492, https://doi.org/10.1016/j.chemosphere.2020.129492.

[6] S. Yan, W. Song, Photo-transformation of pharmaceutically active compounds in the aqueous environment: a review, Environ. Sci. Process. Impacts 16 (2014) 697–720, https://doi.org/10.1039/C3EM00502J.

[7] D. Vione, M. Minella, V. Maurino, C. Minero, Indirect photochemistry in sunlit surface waters: photoinduced production of reactive transient species, Chem. Eur J. 20 (2014) 10590–10606, https://doi.org/10.1002/chem.201400413.

[8] Z. Guo, D. Kodikara, L.S. Albi, Y. Hatano, G. Chen, C. Yoshimura, J. Wang, Photodegradation of organic micropollutants in aquatic environment: importance, factors and processes, Water Res. 231 (2023) 118236, https://doi.org/10.1016/j.watres.2022.118236.

[9] J. Mack, J.R. Bolton, Photochemistry of nitrite and nitrate in aqueous solution: a review, J. Photochem. Photobiol. Chem. 128 (1999) 1–13, https://doi.org/10.1016/S1010-6030(99)00155-0.

[10] K. McNeill, S. Canonica, Triplet state dissolved organic matter in aquatic photochemistry: reaction mechanisms, substrate scope, and photophysical properties, Environ. Sci. Process. Impacts 18 (2016) 1381–1399, https://doi.org/10.1039/C6EM00408C.

[11] X.Z. Niu, J.P. Croué, Photochemical production of hydroxyl radical from algal organic matter, Water Res. 161 (2019) 11–16, https://doi.org/10.1016/j.watres.2019.05.089.

[12] S.L.H. Sandvik, P. Bilski, J.D. Pakulski, C.F. Chignell, R.B. Coffin, Photogeneration of singlet oxygen and free radicals in dissolved organic matter isolated from the Mississippi and Atchafalaya River plumes, Mar. Chem. 69 (2000) 139–152, https://doi.org/10.1016/S0304-4203(99)00101-2.

[13] S. Canonica, T. Kohn, M. Mac, F.J. Real, J. Wirz, U. Von Gunten, Photosensitizer method to determine rate constants for the reaction of carbonate radical with organic compounds, Environ. Sci. Technol. 39 (2005) 9182–9188, https://doi.org/10.1021/es051236b.

[14] L. Wojnárovits, T. Tóth, E. Takács, Rate constants of carbonate radical anion reactions with molecules of environmental interest in aqueous solution : a review, Sci. Total Environ. 717 (2020) 137219, https://doi.org/10.1016/j.scitotenv.2020.137219.

[15] Y.H. Xiao, A. Räike, H. Hartikainen, A.V. Vähätalo, Iron as a source of color in river waters, Sci. Total Environ. 536 (2015) 914–923, https://doi.org/10.1016/j.scitotenv.2015.06.092.

[16] P. Westerhoff, S.P. Mezyk, W.J. Cooper, D. Minakata, Electron pulse radiolysis determination of hydroxyl radical rate constants with suwannee river fulvic acid and other dissolved organic matter isolates, Environ. Sci. Technol. 41 (2007) 4640–4646, https://doi.org/10.1021/es062529n.

[17] S. Yan, Y. Liu, L. Lian, R. Li, J. Ma, H. Zhou, W. Song, Photochemical formation of carbonate radical and its reaction with dissolved organic matters, Water Res. 161 (2019) 288–296, https://doi.org/10.1016/j.watres.2019.06.002.

[18] K.M. Parker, W.A. Mitch, Halogen radicals contribute to photooxidation in coastal and estuarine waters, Proc. Natl. Acad. Sci. U.S.A. 113 (2016) 5868–5873, https://doi.org/10.1073/pnas.1602595113.

[19] B. Ambrose, B. Avant, Y. Han, C. Knightes, T. Wool, Water quality assessment simulation program (WASP8): upgrades to the advanced toxicant module for simulating dissolved chemicals. Nanomaterials, and Solids, US EPA, 2017.

[20] M. Bodrato, D. Vione, APEX (Aqueous Photochemistry of Environmentally occurring Xenobiotics): a free software tool to predict the kinetics of photochemical processes, Environ. Sci. Process. Impacts 16 (2014) 732–740, https://doi.org/10.1039/c3em00541k.

[21] R. Frank, W. Klöpffer, A convenient model and program for the assessment of abiotic degradation of chemicals in natural waters, Ecotoxicol. Environ. Saf. 17 (1989) 323–332, https://doi.org/10.1016/0147-6513(89)90053-5.

[22] R. Zepp, R. Parmar, GCSOLAR.NET User's Manual Calculating Photolysis Rate Constants of Contaminants in Water Version 1.0, US EPA, 2018.

[23] C. Yuan, C. Tebes-Stevens, E.J. Weber, Reaction library to predict direct photochemical transformation products of environmental organic contaminants in sunlit aquatic systems, Environ. Sci. Technol. 54 (2020) 7271–7279, https://doi.org/10.1021/acs.est.0c00484.

[24] C. Yuan, C. Tebes-Stevens, E.J. Weber, Prioritizing direct photolysis products predicted by the chemical transformation simulator: relative reasoning and absolute ranking, Environ. Sci. Technol. 55 (2021) 5950–5958, https://doi.org/10.1021/acs.est.0c08745.

[25] M. Um, L. Fan, O.A.H. Jones, F. Roddick, A comparative study of programs to predict direct photolysis rates in wastewater systems, Sci. Total Environ. 912 (2024) 168921, https://doi.org/10.1016/j.scitotenv.2023.168921.

[26] D. Vione, The modelling of surface-water photoreactions made easier: introducing the concept of 'equivalent monochromatic wavelengths', Water Res. 190 (2021) 116675 https://doi.org/10.1016/j.watres.2020.116675.

[27] Á. García-Gil, J. Marugán, D. Vione, A model to predict the kinetics of direct (endogenous) virus inactivation by sunlight at different latitudes and seasons, based on the equivalent monochromatic wavelength approach, Water Res. 208 (2022) 117837, https://doi.org/10.1016/j.watres.2021.117837.

[28] L. Carena, Á. García-Gil, J. Marugán, D. Vione, Global modeling of lake-water indirect photochemistry based on the equivalent monochromatic wavelength approximation: the case of the triplet states of chromophoric dissolved organic matter, Water Res. 241 (2023) 120153, https://doi.org/10.1016/j.watres.2023.120153.

[29] M.L. Messager, B. Lehner, G. Grill, I. Nedeva, O. Schmitt, Estimating the volume and age of water stored in global lakes using a geo-statistical approach, Nat. Commun. 7 (2016) 13603, https://doi.org/10.1038/ncomms13603.

[30] K. Toming, J. Kotta, E. Uuemaa, S. Sobek, T. Kutser, L.J. Tranvik, Predicting lake dissolved organic carbon at a global scale, Sci. Rep. 10 (2020) 8471, https://doi.org/10.1038/s41598-020-65010-3.

[31] K. Toming, J. Kotta, E. Uuemaa, S. Sobek, T. Kutser, L.J. Tranvik, Predicted Lake Dissolved Organic Carbon at a Global Scale, Zenodo, 2020, https://doi.org/10.5281/zenodo.3452124 [Data set].

[32] B. Lehner, M.L. Messager, HydroLAKES technical documentation version 1.0. https://data.hydrosheds.org/file/technical-documentation/HydroLAKES_TechDoc_v10.pdf, 2016.

[33] X. Zhang, A. Lardizabal, A.I. Silverman, D. Vione, T. Kohn, T.H. Nguyen, J.S. Guest, Global sensitivity analysis of environmental, water quality, photoreactivity, and engineering design parameters in sunlight inactivation of viruses, Environ. Sci. Technol. 54 (2020) 8401–8410, https://doi.org/10.1021/acs.est.0c01214.

[34] NCAR, Quick TUV calculator. http://cprm.acom.ucar.edu/Models/TUV/Interactive_TUV/, 2015.

[35] E. De Laurentiis, M. Minella, V. Maurino, C. Minero, M. Brigante, G. Mailhot, D. Vione, Photochemical production of organic matter triplet states in water samples from mountain lakes, located below or above the treeline, Chemosphere 88 (2012) 1208–1213, https://doi.org/10.1016/j.chemosphere.2012.03.071.

[36] R. Andreozzi, M. Raffaele, P. Nicklas, Pharmaceuticals in STP effluents and their solar photodegradation in aquatic environment, Chemosphere 50 (2003) 1319–1330, https://doi.org/10.1016/S0045-6535(02)00769-5.

[37] P. Avetta, D. Fabbri, M. Minella, M. Brigante, V. Maurino, C. Minero, M. Pazzi, D. Vione, Assessing the phototransformation of diclofenac, clofibric acid and naproxen in surface waters: model predictions and comparison with field data, Water Res. 105 (2016) 383–394, https://doi.org/10.1016/j.watres.2016.08.058.

[38] L. Carena, C.G. Puscasu, S. Comis, M. Sarakha, D. Vione, Environmental photodegradation of emerging contaminants: a re-examination of the importance of triplet-sensitised processes, based on the use of 4-carboxybenzophenone as proxy for the chromophoric dissolved organic matter, Chemosphere 237 (2019) 124476, https://doi.org/10.1016/j.chemosphere.2019.124476.

[39] S. Canonica, H.U. Laubscher, Inhibitory effect of dissolved organic matter on triplet-induced oxidation of aquatic contaminants, Photochem. Photobiol. Sci. 7 (2008) 547–551, https://doi.org/10.1039/b719982a.

[40] J. Wenk, S. Canonica, Phenolic antioxidants inhibit the triplet-induced transformation of anilines and sulfonamide antibiotics in aqueous solution, Environ. Sci. Technol. 46 (2012) 5455–5462, https://doi.org/10.1021/es300485u.

[41] J.L. Packer, J.J. Werner, D.E. Latch, K. McNeill, W.A. Arnold, Photochemical fate of pharmaceuticals in the environment: naproxen, diclofenac, clofibric acid, and ibuprofen, Aquat. Sci. 65 (2003) 342–351, https://doi.org/10.1007/s00027-003-0671-8.

[42] QGIS Development Team, QGIS Geographic Information System, QGIS Association, 2024. http://www.qgis.org.

[43] J. Moreno-SanSegundo, S. Giannakis, S. Samoili, G. Farinelli, K.G. McGuigan, J. Marugán, SODIS potential: a novel parameter to assess the suitability of solar water disinfection worldwide, Chem. Eng. J. 419 (2021) 129889, https://doi.org/10.1016/j.cej.2021.129889.

[44] I. Reda, A. Andreas, Solar position Algorithm for solar radiation applications, NREL Report No. TP-560-34302, Revised January 2008, https://www.nrel.gov/docs/fy08osti/34302.pdf, 2003 (accessed 2022).

[45] F. Calderaro, D. Vione, Possible effects of climate change on surface-water photochemistry. A model assessment of the impact of browning on the photodegradation of pollutants in lakes during summer stratification: epilimnion vs. whole-lake phototransformation, Molecules 25 (2020) 2795, https://doi.org/10.3390/molecules25122795.

[46] J.N. Apell, S. Kliegman, C. Solá-Gutiérrez, K. McNeill, Linking triclosan's structural features to its environmental fate and photoproducts, Environ. Sci. Technol. 54 (2020) 14432–14441, https://doi.org/10.1021/acs.est.0c05121.

[47] S.A. Loiselle, H. Duan, Z. Cao, Characteristics of the underwater light field, in: P. Calza, D. Vione (Eds.), Surface Water Photochemistry, The Royal Society of Chemistry, 2015, pp. 39–59.
[48] S.B. Partanen, K. McNeill, Global corrections to reference irradiance spectra for non-clear-sky conditions, Environ. Sci. Technol. 57 (2023) 2682–2690, https://doi.org/10.1021/acs.est.2c07359.
[49] M. O'Connor, S.R. Helal, D.E. Latch, W.A. Arnold, Quantifying photo-production of triplet excited states and singlet oxygen from effluent organic matter, Water Res. 156 (2019) 23–33, https://doi.org/10.1016/j.watres.2019.03.002.
[50] C. Tixier, H.P. Singer, S. Oellers, S.R. Müller, Occurrence and fate of carbamazepine, clofibric Acid, diclofenac, ibuprofen, ketoprofen, and naproxen in surface waters, Environ. Sci. Technol. 37 (2003) 1061–1068, https://doi.org/10.1021/es025834r.
[51] M.E. Verbyla, J.R. Mihelcic, A review of virus removal in wastewater treatment pond systems, Water Res. 71 (2015) 107–124, https://doi.org/10.1016/j.watres.2014.12.031.
[52] T. Kohn, M.J. Mattle, M. Minella, D. Vione, A modeling approach to estimate the solar disinfection of viral indicator organisms in waste stabilization ponds and surface waters, Water Res. 88 (2016) 912–922, https://doi.org/10.1016/j.watres.2015.11.022.